

# INTERFACIAL CRACKING BETWEEN AN EPOXY-BASED COMPOSITE COATING AND A RIGID SUBSTRATE UNDER THERMAL LOADING

Helezi Zhou<sup>1,2</sup>, Hong-Yuan Liu<sup>2</sup>, Huamin Zhou<sup>1</sup>, Yun Zhang<sup>1</sup>, Xusheng Du<sup>3</sup>, Dong Yan<sup>1</sup>, Haitao Wang<sup>1</sup> and Yiu-Wing Mai<sup>2</sup>

<sup>1</sup> State Key Laboratory of Materials Processing and Die & Mould Technology  
Huazhong University Science and Technology, Wuhan 430074, China

<sup>2</sup> Centre for Advanced Materials Technology (CAMT)  
School of Aerospace, Mechanical and Mechatronics Engineering J07  
The University of Sydney, Sydney, NSW 2006, Australia

<sup>3</sup> Institute of Advanced Wear & Corrosion Resistance and Functional Materials  
Jinan University, Guangzhou, 510632, China

**Keywords:** epoxy-based composites, crack propagation, J-integral, thermo-mechanical stress.

## ABSTRACT

Owing to the difference in thermal expansion of an epoxy coating layer and a substrate, existing pre-cracks/defects in the coating/substrate interface may suffer high thermal stresses in the coating system. Using Finite Element Analysis (FEA) based on ABAQUS, this study showed that pre-cracks initiated at the edge were more severe than those at the centre. Once delamination was triggered by the temperature change induced thermal loading, it propagated quickly along the coating/substrate interface, which was consistent with experimental observations. It was also found that the coating thickness and temperature change magnitudes were important factors affecting the fracture behaviour of the coating. Moreover, incorporation of fillers into an epoxy matrix was found to reduce the driving force (given as stress intensity factor K or J-integral) of an interfacial crack. Hence, the effects of filler parameters such as the elastic modulus, thermal expansion coefficient, volume ratio, aspect ratio and orientation, etc. were conducted to provide useful results for improving the design of epoxy composite coatings for different engineering application.

## 1 INTRODUCTION

Epoxies have been widely used as protective coatings in many engineering applications. They are applied on the surfaces of objects like the metal part of electrical wire, pipelines, aircraft radome and submarines, to prevent them from corroding or rusting in harsh environments. One critical factor of the harsh environments is temperature change [1,2]. Thus, when an aircraft is in service, the temperature difference can be as much as ~100 °C. The mismatch in thermal expansions of an epoxy coating and a metal substrate causes high thermal stresses which may lead to crack initiation and crack growth at the interface between the coating layer and the substrate. Hence, the effects of thermal stresses should be considered in the design of coating materials.

One common method to increase the safety factor is by incorporating fillers into the epoxy coating. The effects of different fillers on the mechanical properties of epoxy composites have been studied for many years. Especially, the capability of nanoparticles to increase the elastic modulus, tensile strength and fracture toughness of bulk epoxy has been confirmed [3,4]. However, the crack driving force, either in terms of stress intensity factor K or J-integral for a coating/substrate interfacial crack, is controlled by the bulk mechanical and physical properties of the coating and the substrate, the bonding between them, the geometric parameters of the coating and the crack tip local stress field influenced by the nearest

fillers. In this study, finite element analyses were conducted to understand the filler effects on the delamination along the coating/substrate interface under thermal stresses.

It is proposed that cracks are initiated from small interfacial defects. J-integral and stress intensity factors K based on linear elastic fracture mechanics were determined to evaluate the interfacial crack tip condition. When the J-integral or K values are larger than the fracture energy or fracture toughness of the interface, the crack would initiate and propagate. The effects of pre-crack location and length, coating thickness, temperature difference and filler parameters were studied in the J and K analyses.

## 2 FINITE ELEMENT ANALYSIS CONSIDERATION

### 2.1 Model formulation

Numerical simulation of the thermo-mechanical stress was conducted using ABAQUS 6.14. Linear elastic fracture mechanics was considered for epoxy matrix in this study [2]. The energy release rate, J-integral, and the stress intensity factors,  $K_I$  and  $K_{II}$ , were calculated.

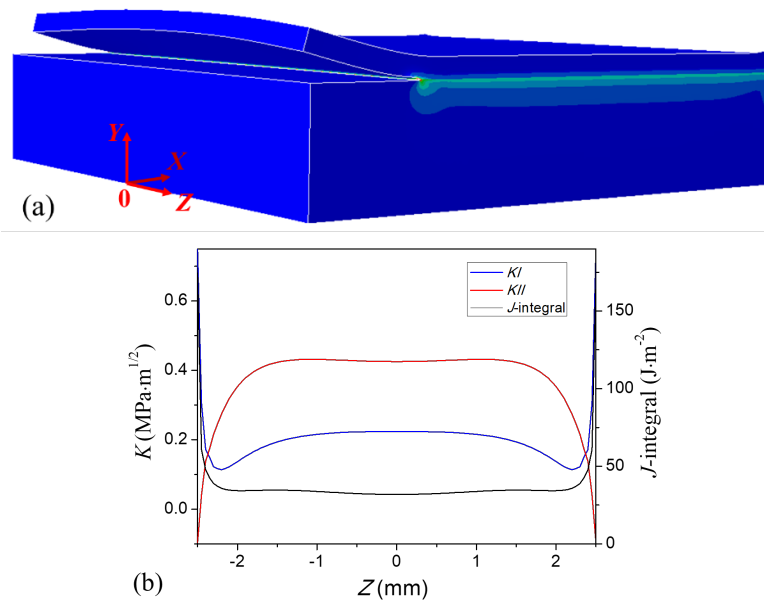


Fig. 1 (a) Schematic diagram of 3-D coating model with Von Mises stress field, and (b) K and J-integral output values from the 3-D model vs Z-direction.

A cuboid shaped substrate ( $5 \times 5 \times 1 \text{ mm}^3$ ) with a thin layer of coating (thickness 0.2 mm) on its top was first considered (see Fig. 1a). An interfacial crack (1 mm in X-direction, 5 mm in Z-direction) was introduced along the edge. The virtual crack extension direction was towards the X-direction along the coating/substrate interface. When the coating sample was cooled down from 120 °C to 20 °C, the coating layer shrank relative to the substrate due to its higher coefficient of thermal expansion (CTE). The calculated J-integral,  $K_I$  and  $K_{II}$  values for the crack tip along the Z-direction are shown in Fig. 1b. Relatively high J-integral and  $K_I$  values are found at the two ends of the interface crack consistent with our experimental observation that crack growth at the edge of the sample was much faster than in the middle area. Also, they reached lower plateau values in the middle area along the Z-direction since the deformation/movement of the coating material was constrained in this direction. Hence, a 2-D model was established (see Fig. 2) with plain strain elements to simplify the 3-D model in the ensuing study.

### 2.2 FEA model

The 2-D model is shown in Fig. 2. The left lower corner of the model was pinned to restrict the freedom of movement. The bottom of the substrate was constrained in the Y-direction ( $U_2=0$ ). All the other edges were free so that the coating layer was allowed to shrink and bend during cooling, stretch

during heating. The interaction type was “general contact” including all surface pairs. The interaction property was “frictionless” and “hard” contact. The coating layer will not penetrate the substrate during heating. The element types are standard and quadratic, plain strain, i.e., CPE8 (an 8-node bi-quadratic plane strain quadrilateral) and CPE6 (a 6-node quadratic plane strain triangle). Detailed meshes with Quad and Tri elements were introduced around the crack tip (as shown by the inserted picture in Fig. 2). The defects/pre-cracks at the coating/substrate interface were specified as seams in the simulation studies (shown as black lines in Fig. 2). The virtual crack extension direction was along the coating/substrate interface (shown as dashed red arrows in Fig. 2).

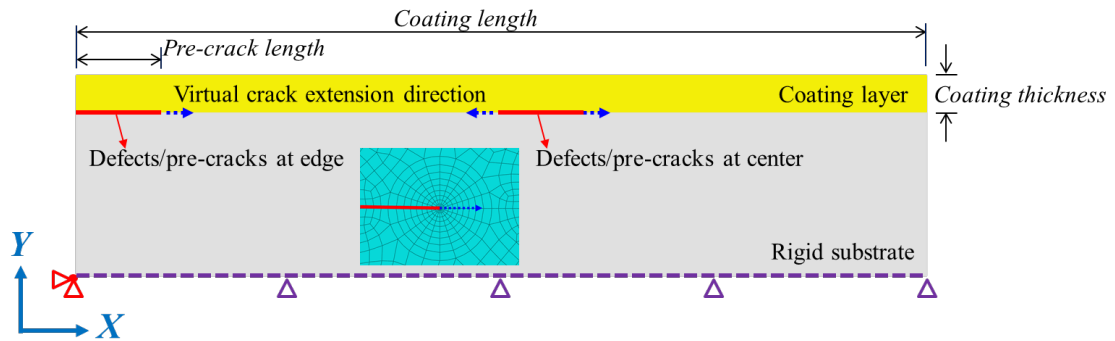


Fig. 2 Schematic of 2-D coating simulation model. The inserted figure illustrates the finite element mesh around the crack tip.

Several assumptions were made in the simulation. These are: (1) thickness of rigid substrate is large enough to ensure that the strain at the bottom of the substrate is near zero; (2) CTE of substrate is taken as zero since CTE values of rigid substrate (glass, stainless steel, etc.) are one order smaller than that of epoxy; (3) coating and substrate are linearly thermo-elastic and are perfectly bonded at the inter -face except at the defined seams; and (5) the interface roughness is not considered. Table 1 lists the material properties of epoxy coating and substrate used in this study. Poisson’s ratio is 0.35.

Materials	$E$ /GPa	CTE/ $K^{-1}$
Pure epoxy	3.22	$6.45 \times 10^{-5}$
Substrate	68	0

Table 1 Material properties of epoxy coating and substrate.

For a coating sample with a pre-crack at the edge, when the environment temperature is decreased, the coating layer shrinks and will form an angle with the substrate. The coating material is subjected to tension and shear. By contrast, when the environment temperature is increased, the coating layer will stretch and cling to the substrate, the interface is under compression and shear,  $K_I$  value is near zero. After the simulations, J-integral and K values around the crack tip will be obtained. If the value approaches the interfacial fracture toughness and/or fracture energy,  $K_{IC}$ ,  $K_{IIC}$  and  $G_{IC}$ , the interfacial crack will propagate. In this study, the interfacial fracture toughness and fracture energy are assumed to be the same as the coating materials.

### 3 Results & Discussion

#### 3.1 Effect of initial defect/pre-crack location and length

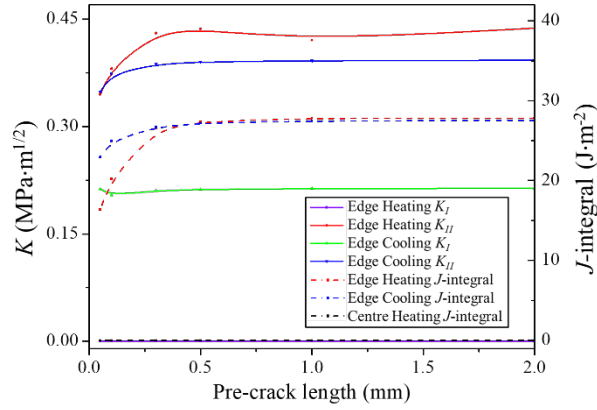


Fig. 3 J-integral and K values from pre-cracks at edge.

Due to imperfect manufacturing processes, defects can exist at the coating and substrate interface. These defects are the locations where the stress concentration and failure may occur. The distribution of those initial defects cannot be predicted. In our calculations, the following case was considered. The initial interfacial defects/pre-cracks with sizes 0.05~2 mm are located at the centre or at the edge of the interface (see Fig. 2). The coating size (thickness×length) is 0.2×5.0 mm<sup>2</sup>. Only thermal stress effect was studied under the temperature difference of 100 °C for pure epoxy and substrate. From the results shown in Fig. 3, K<sub>II</sub> and J-integral values for pre-cracks at the edge increase quickly with increasing length until a small length ~0.5 mm, especially for the heating process, then reach the plateau values at higher pre-crack lengths. Also, independent of heating or cooling, plateau K<sub>II</sub> values are much higher than K<sub>I</sub> (for heating K<sub>I</sub>≈0). However, the J-integral for pre-cracks at the centre (1.4×10<sup>-6</sup> kJ·m<sup>-2</sup> for 2 mm length) is much lower than the critical value. Hence, in later discussions, pre-cracks located at the centre would not be further considered.

### 3.2 Effect of temperature change

A 1.0 mm length pre-crack was defined at the edge of the coating/substrate interface. The coating size is 0.5×5.0 mm<sup>2</sup>. The coating system was cooled down from temperature T to (T-ΔT). The effect of ΔT on the interfacial J-integral is shown in Fig. 4. Clearly, K<sub>I</sub> and K<sub>II</sub> increase linearly but J-integral increases quadratically with increasing ΔT, which are consistent with the K and J-integral equations (see eq.1 and eq.2) [6] below:

$$(\sigma_{22} + \sigma_{12})_{\theta=0} = (K_I + iK_{II})r^{i\epsilon} / \sqrt{2\pi r} \quad (1)$$

$$J = (1 - \beta^2)(K_I^2 + K_{II}^2) / E^* \quad (2)$$

where  $\beta$  and  $E^*$  are constants for given materials.

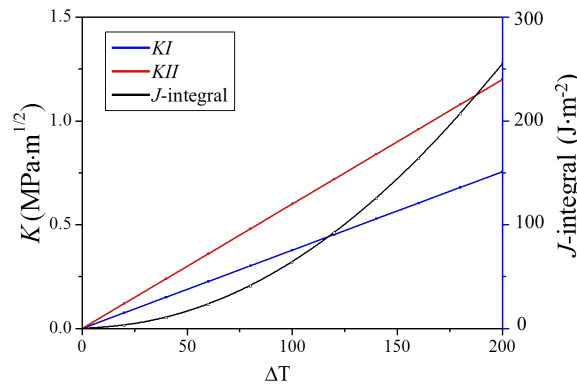


Fig. 4 Effect of ΔT on interfacial K values and J-integral.

### 3.3 Effect of coating thickness

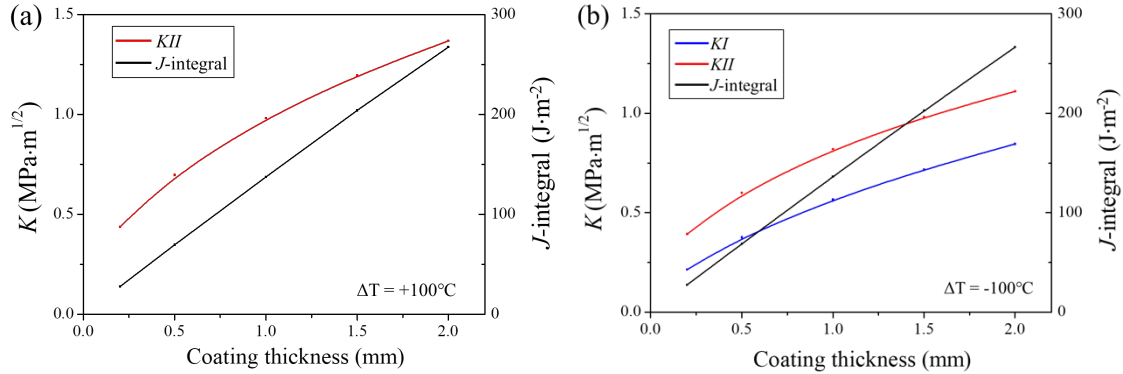


Fig. 5 Effect of coating thickness on interfacial J-integral when the coating system is: (a) heated up from T to (T+100) °C; and (b) cooled down from T to (T-100) °C.

The effect of coating thickness on the interfacial J-integral is shown in Fig. 5. The coating length and edge pre-crack length are 25 and 3.0 mm, respectively. The J-integral increases gradually with the coating thickness. With the same temperature change of  $\pm 100^\circ\text{C}$ , higher  $K_{II}$  values and J-integral are obtained when heating up the coating system (Fig. 5a) than cooling down (Fig. 5b). Indeed, when the coating thickness is 2 mm, the J-integral approaches the fracture toughness of the epoxy matrix, which may lead to crack growth in the epoxy or at the epoxy/substrate interface.

### 3.4 Effects of filler modulus and CTE

To improve the interfacial fracture resistance, round shaped particles (typically 0-D fillers) were first considered to modify the epoxy matrix. These particles are represented in Figure 6 by circles distributed uniformly within the epoxy matrix in the coating layer (thickness  $\times$  coating length =  $0.2 \times 5.0 \text{ mm}^2$ ). The coating/substrate interfacial pre-crack length is 1.0 mm whose tip is located between two fillers. The temperature change is  $-100^\circ\text{C}$ .

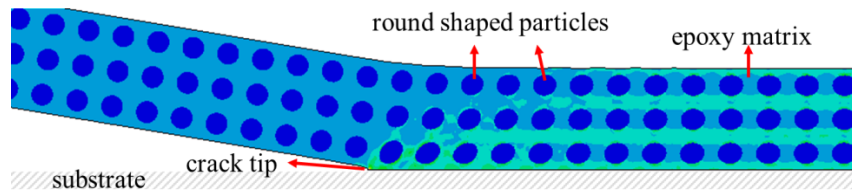


Fig. 6 Schematic for particle modified epoxy composites as coating material with a coating/substrate interfacial crack.

The volume percent and diameter of the particles were 30 vol.% and  $41.2 \mu\text{m}$ , respectively. To study the influence of Young's modulus  $E$  and CTE of particles we assume three sets of values, respectively, giving 9 combinations of material properties as shown in Table 2, which also lists all computed J-integral values for 9 epoxy composite coatings. The lowest J-integral of  $16.4 \text{ J}\cdot\text{m}^{-2}$  is observed for particles with the lowest  $E$  and CTE. J-integral increases to a maximum of  $83.6 \text{ J}\cdot\text{m}^{-2}$  at the highest  $E$  and CTE.

E/GPa	CTE/ $\times 10^{-6} \text{ K}^{-1}$		
	J-integral/ $\text{J}\cdot\text{m}^{-2}$	2.6	64.5
0.05	16.4	17.2	18.2
10	18.4	35.8	69.1
30	20.8	42.0	83.6

\* J-integral for pure epoxy coating is  $27.5 \text{ J}\cdot\text{m}^{-2}$ .

Table 2: Effects of particles  $E$  and CTE on the J-integral.

### 3.5 Effect of filler volume ratio

We have recently studied epoxies incorporated with nano-silica and nano-rubber [3] particles, and obtained their E and CTE values. They can, in theory, be best fitted by Halpin-Tsai's equation and the Rule of Mixtures (ROM) [7], respectively, to determine the E and CTE values of silica and rubber nanoparticles. Here, without performing such regression analysis, we assume (10 GPa,  $2.6 \times 10^{-6} \text{ K}^{-1}$ ) and (50 MPa,  $1.5 \times 10^{-4} \text{ K}^{-1}$ ) from Table 2 as typical (E, CTE) values for 0-D hard and soft fillers, respectively, in order to examine their volume ratio effect on the J-integral at the interface crack.

Other parameters for the coating/substrate system were the same as those used in Section 3.2. That is, coating size ( $0.2 \times 5.0 \text{ mm}^2$ ), pre-crack length (1.0 mm), crack tip (either between two fillers or under the filler), temperature change ( $-100^\circ\text{C}$ ) and particle diameter ( $41.6 \text{ }\mu\text{m}$ ). The particle volume ratio varied from 0 to 30 vol.%.

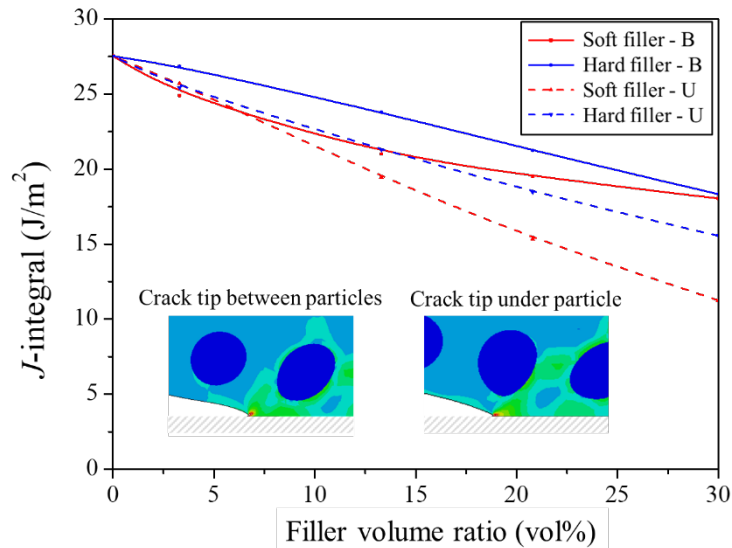


Fig. 7 Effect of 0-D hard or soft filler volume ratio on J-integral.

The influence of filler volume ratio on the J-integral of the interfacial crack is given in Fig. 7. For either hard or soft particle modified epoxies, the J-integral decreases gradually with increasing particle loading. Comparing the four curves, the interfacial J-integral values of crack growth under the particle are lower than those between the particles due to the different stress field around the crack tip (see insets in Fig. 7). Also, the soft particles performed better than the hard particles. For example, when the crack tip is under the particle, with 30 vol.% soft particles in epoxy, the J-integral is 41% of the corresponding value of pure epoxy (see "Soft filler - U" curve). In addition, by incorporating hard or soft particles into epoxy, the fracture toughness of epoxy composites can be significantly increased [3,8], that is, the thresholds for crack growth can be increased. It is noted, however, that the calculated J-integral values in this Section are small compared to the composite fracture energy [3]. But with increasing coating thickness and value of temperature change (see Figs. 3 and 4), the J-integral will increase rapidly and approach the fracture energy of the coating materials or coating/substrate interface.

### 3.6 Effect of particle aspect ratio

1-D particles with different aspect ratio were considered here. The length and width of the particles will change but the area of each particle is kept constant as the 0-D particles ( $0.25 \times \pi \times 41.2^2 \text{ }\mu\text{m}^2$ ). The particle aspect ratio was calculated by length/width. We also assume  $E=10 \text{ GPa}$  [9] and  $\text{CTE}=2.6 \times 10^{-6} \text{ K}^{-1}$  [10, 11] for these typical 1-D particles, which were dispersed parallel to the coating/epoxy interface (shown as H-1-D particles in Fig. 8). The other parameters are: coating size ( $0.2 \times 5.0 \text{ mm}^2$ ), pre-crack length (1.0 mm), crack tip location (between fillers), temperature change ( $\pm 100^\circ\text{C}$ ), and particle volume ratio (30 vol. %).

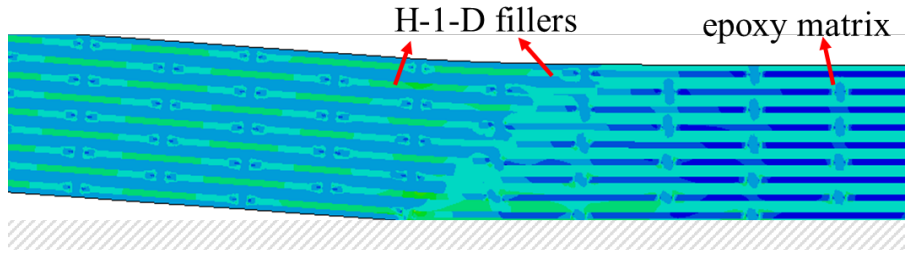


Fig. 8 Schematic of H-1-D fillers dispersed in epoxy matrix.

The influence of particle aspect ratio on J-integral is given in Fig. 9. Compared to neat epoxy and hard 0-D particle ( $d=41.2 \mu\text{m}$ ) modified epoxy, 1-D particles further decrease the J-integral of the coating system. Moreover, the J-integral is decreased with increasing particle aspect ratio under both increasing and decreasing temperature. However, J-integral is only decreased slightly when the aspect ratio is changed from 20 to 70.

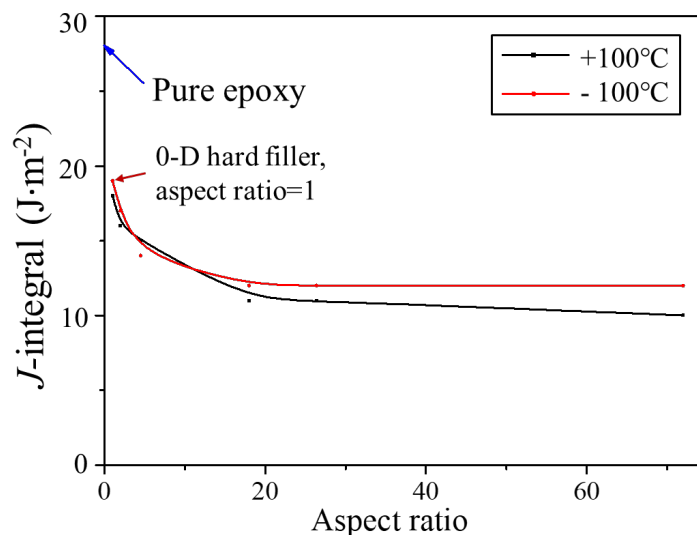


Fig. 9 J-integral of coating system *versus* particle aspect ratio.

### 3.7 Effect of particle orientation

For 1-D particle modified polymer composites, besides the aspect ratio, orientation is an important geometric factor influencing the mechanical performance [12]. Different to Section 3.6, the 1-D particles are transverse to the coating/substrate interface (see Fig. 10). Other parameters are: coating size ( $0.2 \times 5.0 \text{ mm}^2$ ), pre-crack length (1.0 mm), crack tip location (between fillers), temperature change ( $\pm 100 \text{ }^\circ\text{C}$ ), particle volume ratio (30 vol. %), 1-D particle size ( $185 \times 7.2 \mu\text{m}^2$ ), and 1-D particle properties ( $E=10 \text{ GPa}$ ,  $\text{CTE}=2.6 \times 10^{-6} \text{ K}^{-1}$ ).

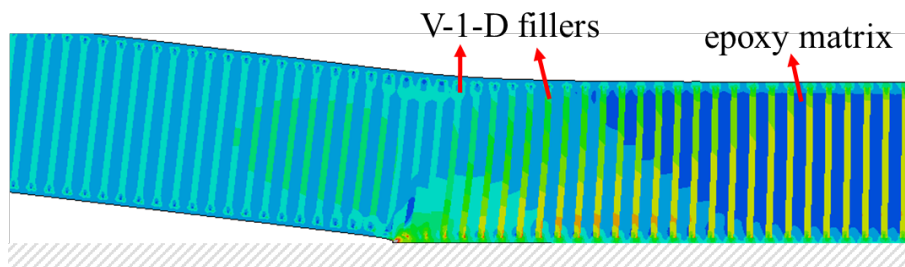


Fig. 10 Schematic of V-1-D fillers dispersed in epoxy matrix.

The J-integral of the coating/substrate interfacial crack with 1-D particles was compared with pure epoxy and 0-D particles modified epoxy coatings (see Table 3). Clearly, the J-integrals were slightly decreased by the incorporation of V-1-D particles in epoxies compared to pure epoxy. This might be

caused by the V-1-D particles unable to efficiently prohibit the deformation of the coating layer. The J-integral values at the interface crack are higher when the 1-D particles are vertical to the interface.

Temp. change	Particles	Control	0-D	V-1-D	H-1-D
	J-integral/J·m <sup>-2</sup>	(no particles)			
-100°C		27.5	18.4	25.5	10.6
+100°C		27.5	18.9	26.7	12.0

Table 3 Effect of 0-D and 1-D particles in epoxy matrix on J-integral

#### 4 CONCLUSIONS

In this study, the effects of some parameters on the coating/substrate interfacial thermal stress have been analysed. J-integral is applied to evaluate the interfacial crack tip condition. Lower J-values mean that it is harder to cause delamination at the interface. The major findings are: (a) J-integral increases with increasing coating thickness and temperature change value; (b) particles with lower E and CTE modified epoxies give lower J-integral values; (c) nanoparticles (e.g., 0-D hard filler, 0-D soft filler, 1-D filler) decrease the coating/substrate interfacial J-integral values with increasing filler loading; and (d) particles with large aspect ratio and parallel to the coating/substrate interface decrease significantly the interfacial J-integral values. It is expected that these results can help understand the failure of epoxy composites coating system better and improve its design towards enhanced performance.

#### ACKNOWLEDGEMENTS

We acknowledge the financial support from the National Natural Science Foundation Council of China for the Major International Joint Research Project (Grant No. 51210004).

#### REFERENCES

- [1] A.A.O. Tay, K.Y. Goh, A study of delamination growth in the die-attach layer of plastic IC packages under hygrothermal loading during solder reflow, *IEEE Trans. Device Mater. Reliab.* 3 (2003) 144–151.
- [2] A.A.O. Tay, L. T. Y., Influence of temperature humidity and defect location on delamination in plastic IC packages, *IEEE Trans. Components Packag. Technol.* 22 (1999) 512–518.
- [3] H.-Y. Liu, G.T. Wang, Y.-W. Mai, Y. Zeng, On fracture toughness of nano-particle modified epoxy, *Compos. Part B Eng.* 42 (2011) 2170–2175.
- [4] H.-Y. Liu, G. Wang, Y.-W. Mai, Cyclic fatigue crack propagation of nanoparticle modified epoxy, *Compos. Sci. Technol.* 72 (2012) 1530–1538.
- [5] E.H. Wong, S.W. Koh, K.H. Lee, K.-M. Lim, T.B. Lim, Y.-W. Mai, Advances in vapor pressure modeling for electronic packaging, *IEEE Trans. Adv. Packag.* 29 (2006) 751–759.
- [6] ABAQUS 6.14, 11.4.2 Contour integral evaluation, in: *Abaqus Anal. User's Man.*, 2014.
- [7] H.T. Vo, M. Todd, F.G. Shi, A.A. Shapiro, M. Edwards, Towards model-based engineering of underfill materials: CTE modeling, *Microelectronics J.* 32 (2001) 331–338.
- [8] L.-C. Tang, H. Zhang, S. Sprenger, L. Ye, Z. Zhang, Fracture mechanisms of epoxy-based ternary composites filled with rigid-soft particles, *Compos. Sci. Technol.* 72 (2012) 558–565.
- [9] A.P. Bathija, *Elastic properties of clays*, Colorado School of Mines, 2009.
- [10] N. Sheng, *Multiscale micromechanical modeling of the thermal/mechanical properties of polymer/clay nanocomposites*, Massachusetts Institute of Technology, 2006.
- [11] Culbertson W. Ross, *Thermal expansion of clay building bricks*, 1941.
- [12] C. Lu, Y.-W. Mai, Influence of aspect ratio on barrier properties of polymer-clay nanocomposites, *Phys. Rev. Lett.* 95 (2005) 1–4.